

Electronic Supplementary Information (ESI)

for

Sensitive colorimetric assay of T4 DNA ligase by integrating the oxidase nanozyme of $\text{LaMnO}_{3.26}$ coupled with hyperbranched amplification reaction

Aohuan Guo, Jie Sun, Menghua Yan, and Guang-Li Wang*

Key Laboratory of Synthetic and Biological Colloids (Ministry of Education), School
of Chemical and Material Engineering, Jiangnan University, Wuxi 214122, China.

* Corresponding author: Guang-Li Wang

*E-mail: glwang@jiangnan.edu.cn

Table of Contents

Materials and reagents	S3
Instruments	S4
Fig. S1 Characterization of LaMnO _{3.26} nanomaterials.....	S5
Fig. S2 Optimization of LaMnO _{3.26} mimetic oxidase activity.....	S5
Fig. S3 Catalytic activity variation of LaMnO _{3.26} in 30 days.....	S6
Table S1. Comparison of the kinetic parameters between LaMnO _{3.26} and other reported nanomaterials.....	S6
Fig. S4 Absorption spectra of oxTMB in the presence of different substances.....	S7
Fig. S5 Dispersion state of the nanozyme under different substances.....	S7
Fig. S6 TEM image of untreated and treated LaMnO _{3.26} by PPI.....	S8
Fig. S7 IR and Raman spectra of LaMnO _{3.26} before and after PPI treatment and the complex structure diagram of PPI and LaMnO _{3.26}	S8
Fig. S8 XPS survey spectra of untreated and PPI treated LaMnO _{3.26}	S9
Fig. S9 Effect of PPI concentration on the oxidation of TMB by LaMnO _{3.26} and the selectivity of PPI.....	S9
Fig. S10 Optimization of biological reaction concentration.....	S10
Fig. S11 Optimization of biological reaction time.....	S10
Table S2. Comparison of detection methods.....	S11
Table S3. Recovery of T4 DNA ligase in human serum samples.....	S11
References	S12

Materials and reagents.

La(NO₃)₃·6H₂O, Mn(CH₃COO)₂·4H₂O, ethylenediaminetetraacetic acid (EDTA), citric acid monohydrate, ammonium hydroxide aqueous solution (NH₄OH), adenosine triphosphate (ATP), sodium pyrophosphate decahydrate (PPi), sodium phosphate (Pi), p-benzoquinone, t-butanol, histidine, triethylenediamine, and tris(hydroxymethyl)aminomethane (Tris) were purchased from Sinopharm Chemical Reagent Co., Ltd. (Shanghai, China). 3,3',5,5'-Tetramethylbenzidine (TMB), 2,2'-azinobis(3-ethylbenzothiazoline-6-sulfonic acid ammonium salt) (ABTS), 2,2,6,6-tetramethylpiperidine (TEMP), and 5,5-dimethyl-1-pyrroline N-oxide (DMPO) were purchased from Inokai Technology Co., Ltd. (Beijing, China). T4 DNA ligase, dATP, ammonium persulfate (APS), N,N,N',N'-tetramethylethylenediamine, and Acryl/Bis 30% solution (29:1) were purchased from Sangon Biotechnology Co., Ltd. (Shanghai, China). Terminal transferase (TdT) and its 10×TdT buffer (50 mM potassium acetate, 20 mM tris-acetate, 10 mM magnesium acetate, pH 7.9@25°C), and endonuclease IV (Endo IV) were bought from New England Biolabs (Ipswich, USA). Bovine serum albumin (BSA), polymerase, T4 polynucleotide kinase (T4 PNK), glucose oxidase (GOx), lysozyme, trypsin, thrombin, E. coli ligase, and superoxide dismutase (SOD) were obtained from Sigma-Aldrich Corporation (St. Louis, MO, USA). All solutions were prepared with ultrapure water (18 MΩ/cm) provided from a Milli-Q purification system.

All oligonucleotides were HPLC-purified and synthesized by Sangon Biotechnology Co., Ltd. (Shanghai, China). The sequences of the oligonucleotides were listed as follows:

Hairpin DNA: 5'-PO₄-TAT AGC TCA ATC GCA CTA GCT ATA TAT AGC TAA CCA CTA ACA GCT ATA-3';

Assistant probe: 5'-PO₄-TTT TTT TTT TTT TTT TTT TTX TTT TT-NH₂-3' (The X in the assistant probe indicates the abasic site mimic).

Instruments

The X-ray diffraction (XRD) pattern was obtained with a D8 Advance X-ray diffractometer using the Cu K α radiation (Brook AXS, Germany). Scanning electron microscopy (SEM) images were determined by a Hitachi S-4800 high resolution scanning electron microscope (Hitachi, Japan). Transmission electron microscope (TEM) images were performed by a JEM-2100 plus transmission electron microscope (Hitachi, Japan). Fourier transform infrared (FT-IR) spectra were recorded on a FALA-2000104 spectrometer (Boman, Canada). The Raman spectra were received on an In Via Raman microscope spectrometer (Renishaw, UK) with the laser excitation wavelength fixed at 785 nm. The X-ray photoelectron spectra (XPS) were acquired with an Axis supra spectrometer (Kratos, UK). UV–vis absorption spectroscopic measurements for solutions were carried out using a TU–1901 spectrophotometer (Puxi, China). The absorption experiments for the detection of T4 DNA ligase were carried out on 96–well plates with a SpectraMax M5 microplate reader (Molecular Devices, USA).

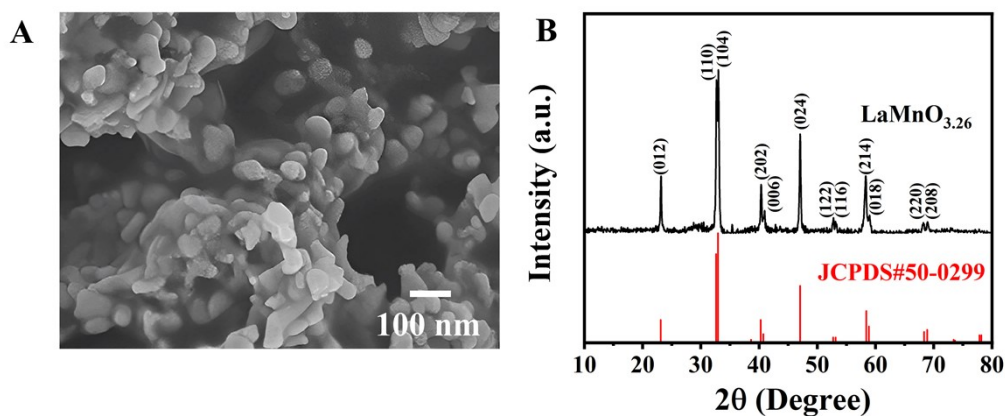


Fig. S1 (A) SEM image and (B) XRD pattern of the synthesized $\text{LaMnO}_{3.26}$.

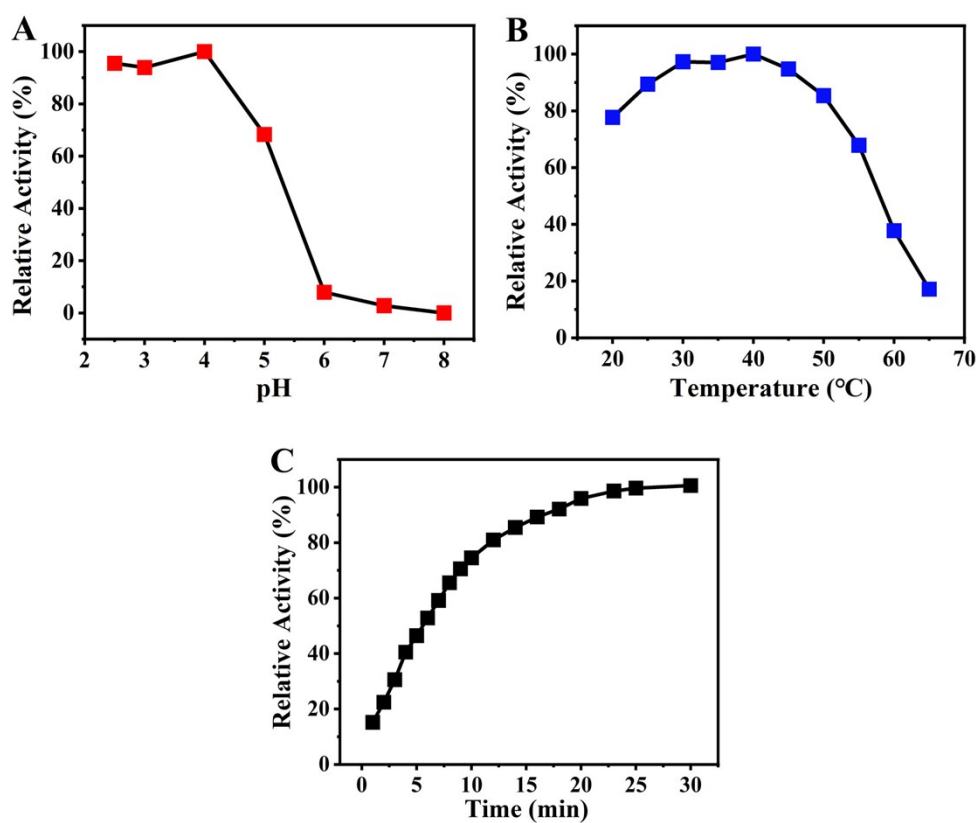


Fig. S2 Relative catalytic activity of $\text{LaMnO}_{3.26}$ mimetic oxidase at (A) different pH of reaction solutions, (B) different temperatures, and (C) different reaction times.

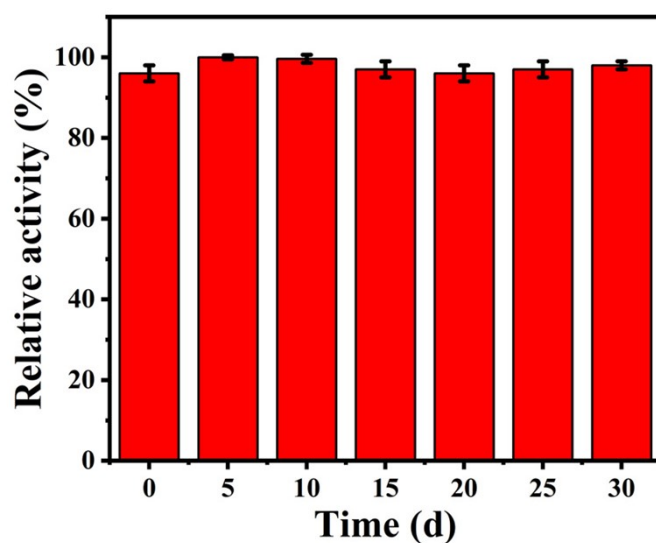


Fig. S3 Catalytic activity variations of LaMnO_{3.26} nanozyme in 30 days. Error bars represent the standard deviation (SD) for three measurements.

Table S1. Comparison of the kinetic parameters between LaMnO_{3.26} and other reported nanomaterials

Materials	K _m (mM)	V _{max} (10 ⁻⁸ M•S ⁻¹)	Reference
NiPd hNPs	0.110	1.52	1
CoMo hybrids	0.177	19.5	2
NiCo ₂ O ₄	0.127	0.127	3
3-CoV MMOs	0.444	9.5	4
Au-PtNCs	0.362	13.6	5
Nanoceria	0.42	10.0	6
LaMnO _{3.26}	0.071	21.9	This work

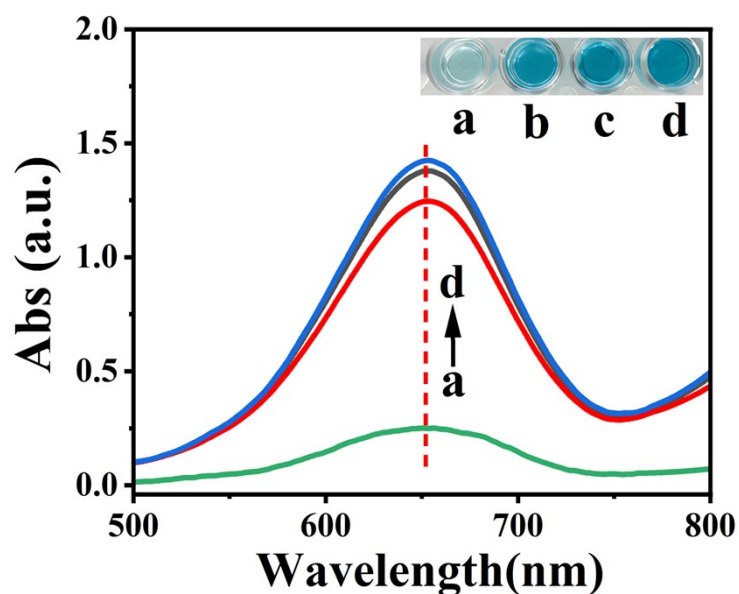


Fig. S4 Absorption diagram of the nanozyme mediated catalytic system when in the presence of different substances: (a) PPI, (b) ATP, (c) Pi, and (d) control. The inset shows the corresponding colors of the reaction solutions. Reaction conditions: the concentration of PPI is 10 mM and the concentrations of ATP and Pi are 100 mM.

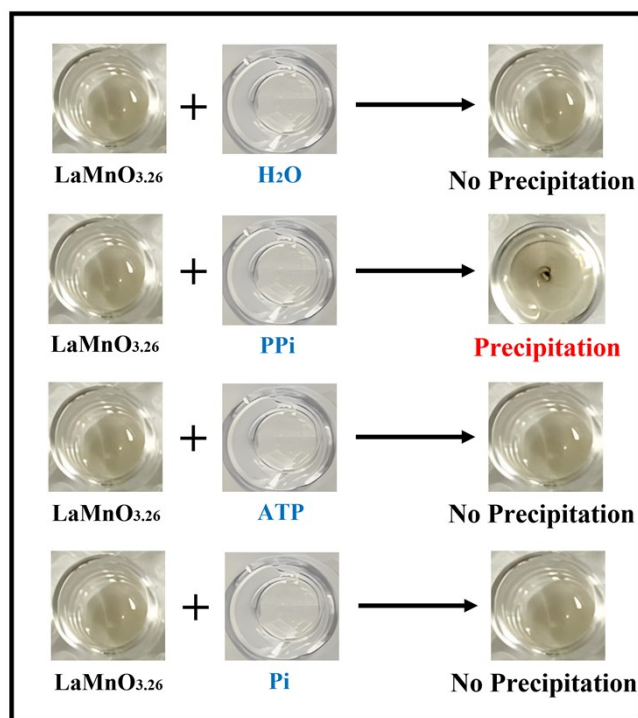


Fig. S5 Graphs of the changes of dispersion state of the $\text{LaMnO}_{3.26}$ nanozyme after mixing with different substances.

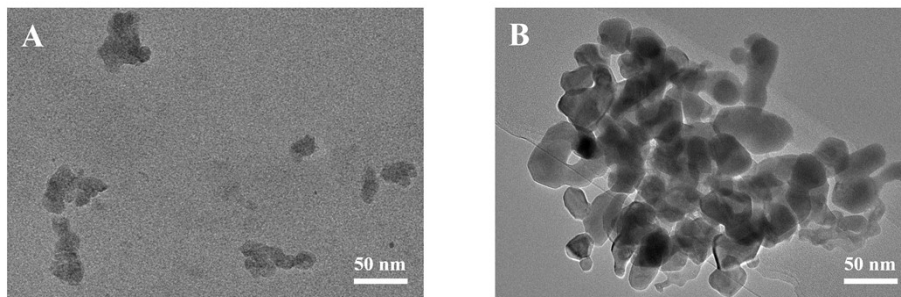


Fig. S6 TEM images of the $\text{LaMnO}_{3.26}$ nanomaterials (A) before and (B) after mixed with PPI.

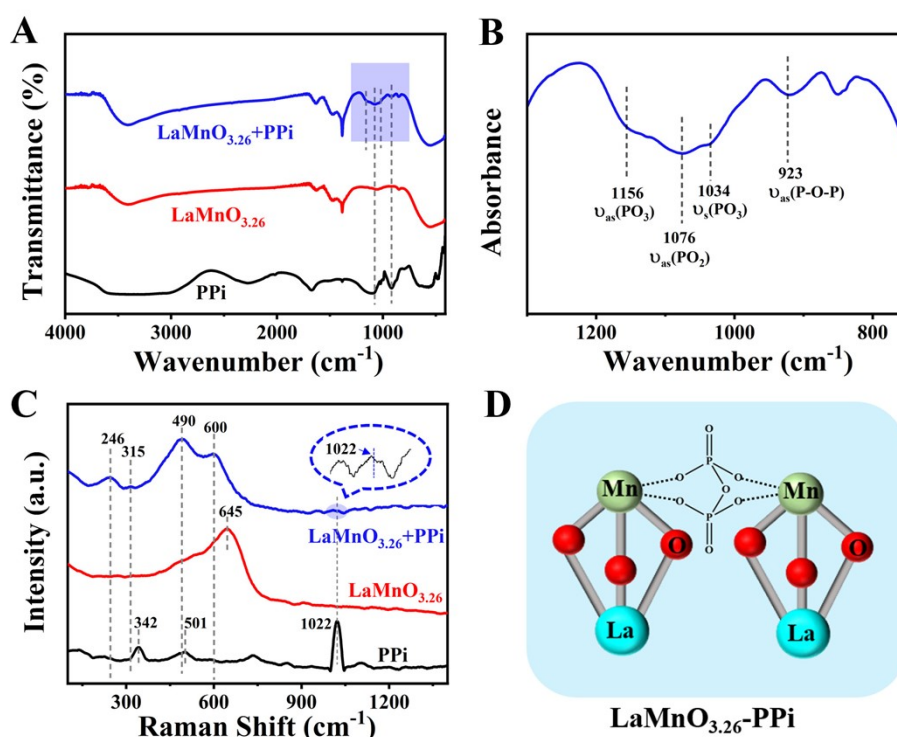


Fig. S7 (A) FT-IR spectra of different samples, (B) detailed IR spectra of the purple shaded part in (A), (C) Raman spectra of different samples, (D) Schematic diagram of the structure of PPI complexed with $\text{LaMnO}_{3.26}$.

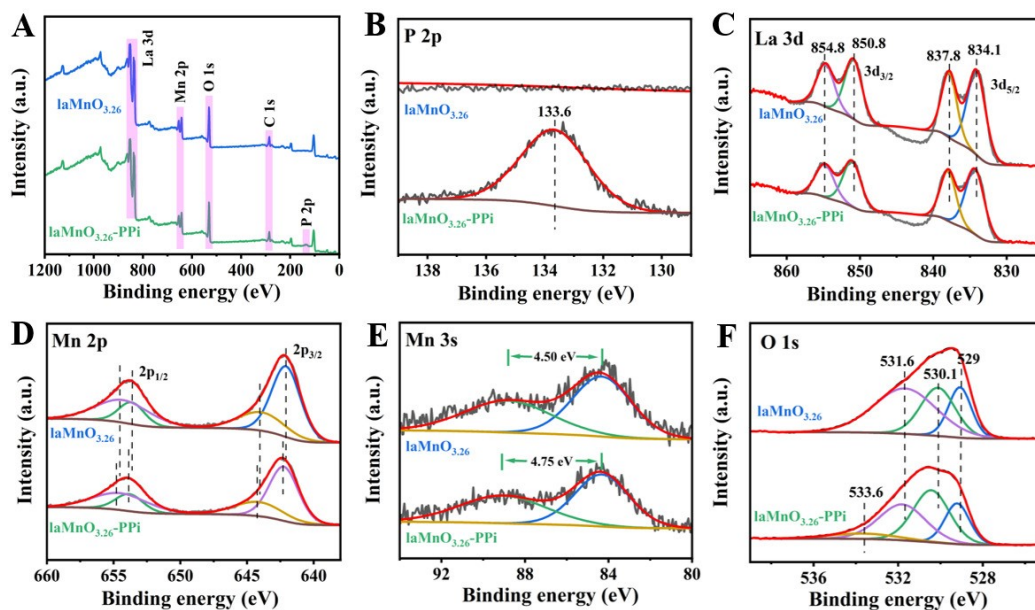


Fig. S8 (A) XPS survey spectra of $\text{LaMnO}_{3.26}$ and PPI treated $\text{LaMnO}_{3.26}$. High-resolution XPS spectra of (B) P 2p, (C) La 3d, (D) Mn 2p, (E) Mn 3s, and (F) O 1s of $\text{LaMnO}_{3.26}$ and PPI treated $\text{LaMnO}_{3.26}$.

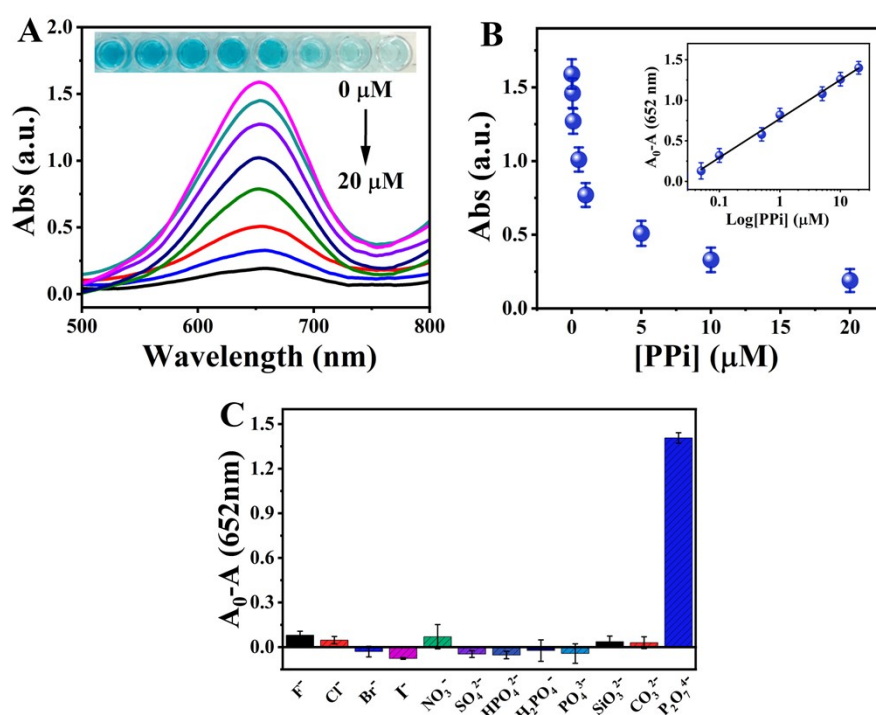


Fig. S9 (A) Effect of PPI concentration on the oxidation of TMB by $\text{LaMnO}_{3.26}$ (PPI concentrations of 0, 0.05, 0.1, 0.5, 1, 5, 10 and 20 μM), (B) Linearity responses for PPI,

(C) Effects of various interfering anions on the catalytic oxidation of TMB by $\text{LaMnO}_{3,26}$. Error bars indicate the standard deviation of the three replicate measurements. A and A_0 are the absorbance intensities of the detection system in the presence and absence of PPI, respectively.

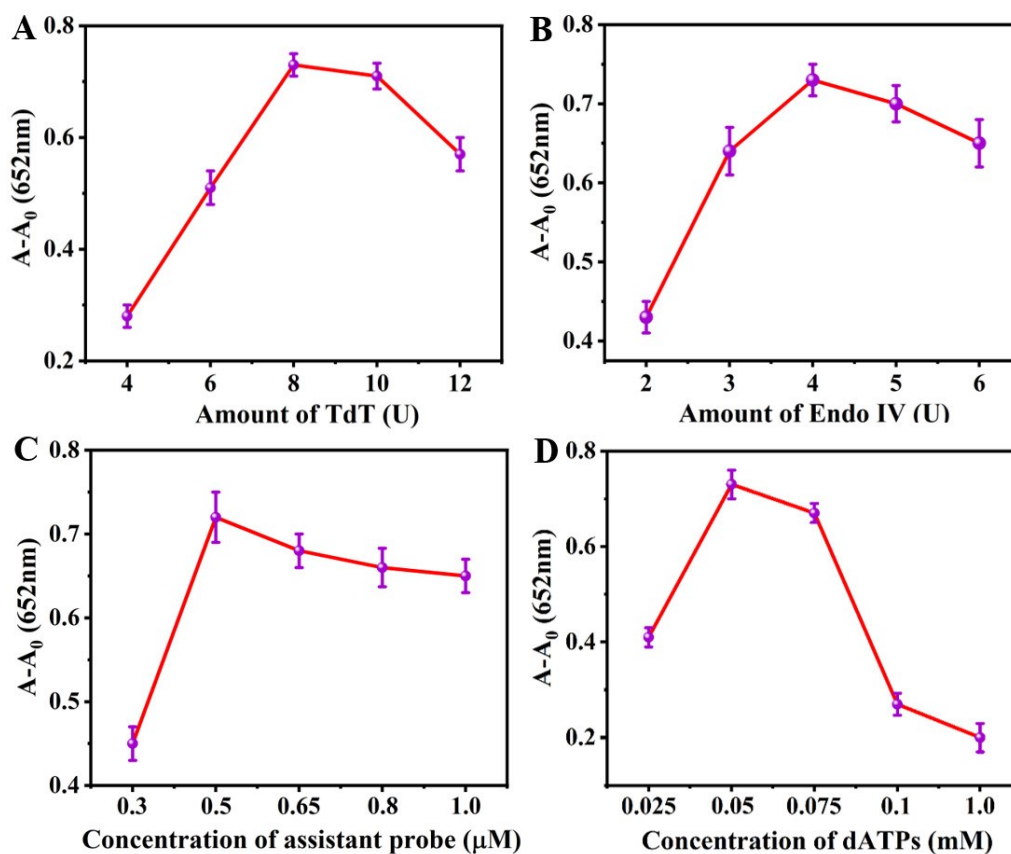


Fig. S10 Absorption increment ($A - A_0$) values versus the concentration of (A) TdT, or (B) Endo IV, or (C) assistant probe, or (D) dATPs. A and A_0 are the absorbance intensities of the detection system in the presence and absence of T4 DNA ligase, respectively. The T4 DNA ligase concentration is 10 U/mL. Error bars indicate the standard deviation of three independent experiments.

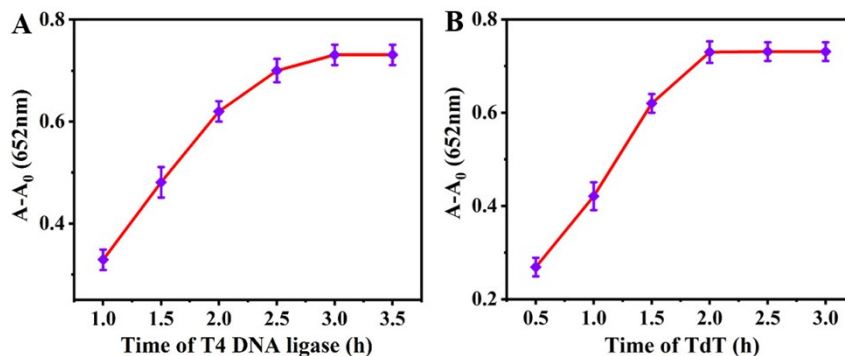


Fig. S11 Influence of (A) ligation time of T4 DNA ligase, and (B) amplification time of TdT on the response of the detection system. A and A₀ are the absorbance intensities in the presence and absence of T4 DNA ligase, respectively. Error bars indicate the standard deviation of three independent experiments.

Table S2. Comparison with other reported methods for the detection of T4 DNA ligase.

Method	Linear Range (U/mL)	LOD (U/mL)	Reference
Fluorescence	0~2.5	1.2×10^{-2}	7
Electrochemical	$5.0 \times 10^{-3} \sim 5$	2.5×10^{-3}	8
Colorimetry	0.2~5	0.2	9
Colorimetry	$4.8 \times 10^{-3} \sim 6$	1.6×10^{-3}	This work

Table S3. Recovery of T4 DNA ligase in the diluted human serum samples (n=4).

Samples	Spiked amount (U/mL)	Detected amount (U/mL)	Recovery (%)	RSD (%)
1	0.03	0.03±0.001	103.3	3.3
2	0.15	0.15±0.003	102.0	2.0
3	0.60	0.65±0.041	108.3	6.3
4	1.00	0.98±0.025	98.0	2.5

References

- 1 Q. Wang, L. Zhang, C. Shang, Z. Zhang, S. Dong, *Chem. Commun.*, 2016, **52**, 5410–5413.
- 2 Y. Ding, G. Wang, F. Sun, Y. Lin, *ACS Appl. Mater. Interfaces*, 2018, **10**, 32567–32578.
- 3 L. Su, W. Dong, C. Wu, Y. Gong, Y. Zhang, L. Li, G. Mao, S. Feng, *Anal. Chim. Acta*, 2017, **951**, 124–132.
- 4 Y. Wang, C. Chen, D. Zhang, J. Wang, *Appl. Catal. B*, 2020, **261**, 118256.
- 5 J. Feng, P. Huang, F. Wu, *Analyst*, 2017, **142**, 4106.
- 6 H. Cheng, S. Lin, F. Muhammad, Y. W. Lin, H. Wei, *ACS Sens.*, 2016, **1**, 1336–1343.
- 7 Y. Guo, Q. Wang, Z. Wang, X. Chen, L. Xu, J. Hu, R. Pei, *Sens. Actuators B Chem.*, 2015, **214**, 50–55.
- 8 X. Y. Wang, P. Dong, W. Yun, Y. Xu, P. G. He, Y. Z. Fang, *Talanta*, 2010, **80**, 1643-1647.
- 9 K. Y. He, W. Li, Z. Nie, Y. Huang, Z. L. Liu, L. H. Nie, S. Z. Yao, *Chem. Eur. J.*, 2012, **18**, 3992-3999.